

## **JGR** Atmospheres



### RESEARCH ARTICLE

10.1029/2024JD041723

### **Key Points:**

- Initial TP land surface warming can generate a local near-surface PV positive center and expand downstream within the first prediction week
- The downstream cyclonic anomaly and increased rainfall can be maintained for 3 weeks in prediction by a positive feedback
- The study confirmed the effect of TP initial thermal condition on the MLYR prediction ahead of 3 weeks in Mei-yu season (peak summer)

#### **Supporting Information:**

Supporting Information may be found in the online version of this article.

#### Correspondence to:

J. Yang, yangjing@bnu.edu.cn

#### Citation:

Fan, Y., Yang, J., Bao, Q., Ma, T., Wu, G., Xue, Y., et al. (2024). How does the Tibetan plateau land thermal initial condition influence the subseasonal prediction of 2020 record-breaking Mei-yu rainfall. *Journal of Geophysical Research: Atmospheres*, *129*, e2024JD041723. https://doi.org/10.1029/2024JD041723

Received 4 JUN 2024 Accepted 8 OCT 2024

## How Does the Tibetan Plateau Land Thermal Initial Condition Influence the Subseasonal Prediction of 2020 Record-Breaking Mei-Yu Rainfall

Yalan Fan<sup>1</sup>, Jing Yang<sup>1</sup>, Qing Bao<sup>2</sup>, Tingting Ma<sup>2</sup>, Guoxiong Wu<sup>2</sup>, Yongkang Xue<sup>3</sup>, Chunxiang Shi<sup>4</sup>, Yimin Liu<sup>2</sup>, and Xin Qi<sup>5</sup>

<sup>1</sup>Key Laboratory of Environmental Change and Natural Disasters of Ministry of Education/Faculty of Geographical Science, Beijing Normal University, Beijing, China, <sup>2</sup>State Key Laboratory of Numerical Modeling for Atmospheric Sciences and Geophysical Fluid Dynamics (LASG), Institute of Atmospheric Physics, Chinese Academy of Sciences, Beijing, China, <sup>3</sup>Department of Geography, University of California Los Angeles, Los Angeles, CA, USA, <sup>4</sup>National Meteorological Information Center, China Meteorological Administration, Beijing, China, <sup>5</sup>Frontiers Science Center for Deep Ocean Multispheres and Earth System (FDOMES), Ocean University of China, Qingdao, China

Abstract Accurate subseasonal prediction of heavy rainfall is helpful for disaster mitigation but challenging. The land thermal condition of Tibetan Plateau (TP), usually with climate memory ranging from weeks to seasons, has been seen as a potential predictability source for subseasonal prediction. Aiming at 2020 record-breaking Mei-yu rainfall, this study attempts to investigate whether and how the influence of initial TP surface thermal condition near late June influences the July rainfall prediction over the Middle and Lower Yangtze River Region (MLYR), based on two contrasting prediction experiments using a global climate ensemble prediction system. The results show that the most distinguishable change in the downstream prediction in July is the anomalous low-tropospheric cyclone and the associated increased rainfall over MLYR corresponding to the warmer initial condition of surface TP. Influenced by the invasion of the positive potential vorticity (PV) center that generated over TP and propagated eastward, this low-level cyclone anomaly over MLYR is formed within the first week of prediction, and persists for the next 3 weeks maintained by the positive feedback between the low-level cyclone and middle-tropospheric latent heating over MLYR in the prediction. This study confirmed the significant effect of TP initial thermal condition on downstream prediction ahead of 3 weeks during the Mei-yu season (peak summer) with strong land-atmosphere coupling over TP.

Plain Language Summary Based on two contrasting prediction experiments using a global climate ensemble prediction system, this study exhibits that changing the initial thermal condition over Tibetan Plateau (TP) surface can significantly influence the subseasonal prediction of rainfall over Middle and Lower Yangtze River Region (MLYR) in Mei-yu season. After the TP land surface warming at the initial time of prediction, a low-level cyclonic and increased rainfall appears within the first week of prediction and persists for the next 3 weeks maintained by the positive feedback between the low-level cyclone and middle-tropospheric latent heating over MLYR. This study confirmed the effect of initial land thermal condition over TP on the MLYR prediction ahead of 3 weeks during Mei-yu season (peak summer) with strong land-atmosphere coupling over TP.

### 1. Introduction

In recent years, the frequency of extreme precipitation events has increased significantly (O'Gorman, 2015; IPCC, 2021; Zhou & Qian, 2021), which has caused huge losses in human life and economies (Fu et al., 2022; Lesk et al., 2016; Wei et al., 2020). Accurate subseasonal prediction for heavy rainfall is increasingly important for both early warning systems and risk mitigation (White et al., 2015). However, subseasonal prediction has lower prediction skill compared to weather forecast (shorter than 7 days) and climate prediction (longer than 2 months) (Robertson et al., 2015). The barriers for increasing subseasonal prediction skill are not only the uncertain predictability sources on this time scale but also the unclarified effects from the near-surface boundary condition as well as the initial conditions (Liang & Lin, 2018; Qi & Yang, 2019; Vitart et al., 2017). Therefore, recognizing the effect of initial meteorological conditions on the subseasonal prediction is crucial but challenging for improving the subseasonal prediction.

© 2024. The Author(s).

This is an open access article under the terms of the Creative Commons

Attribution License, which permits use, distribution and reproduction in any medium, provided the original work is properly cited.

Earth surface condition serves as one of the important initial conditions for subseasonal prediction, which usually contains longer climate "memory" than atmosphere (Mariotti et al., 2018). Based on observational diagnosis and numerical simulations, previous studies have demonstrated that compared with sea ice, snow and ocean whose memories concentrate on the seasonal-to-annual time scale (He et al., 2018; Sobolowski et al., 2010; Wu & Francis, 2019), the memory of land surface condition is more distinguishable in subseasonal time scale from weeks to season (Dirmeyer et al., 2019; Seneviratne et al., 2010). For example, by taking numerical experiments of general circulation model, Yeh et al. (1984) addressed that the soil moisture anomalies associated with irrigation can persist for at least 2 months in the latitude zones that are initially saturated with moisture. Based on the top 2-m soil depth data sets, Amenu et al. (2005) found that the memory of land subsurface temperature/moisture is about 53 days/3 months measured by the e-folding time of the soil temperature/moisture anomalies. Liu et al. (2020) demonstrated that the land surface and subsurface temperature anomaly over the Tibetan Plateau (TP) during spring exhibit a memory of 1–3 months by calculating the autocorrelation of the anomalous time series based on observational data.

In addition, the initialization of land surface condition has been found to have a significant influence on the subseasonal prediction. For instance, by comparing the differences of precipitation prediction skill between the results with and without realistic land initialization, Koster et al. (2004, 2010) demonstrated that precise land initialization can improve the prediction skill of precipitation and air temperature out to a 30-day lead over North America. Calculating the year-to-year correlation coefficients between predictions and observations, Yamada and Pokhrel (2019) showed that improved land initialization, incorporating more accurate simulations of global irrigation and groundwater withdrawals, can enhance the 40-day lead air temperature prediction skill for the majority of regions in the United States in boreal summer. However, the accuracy and realism of land surface conditions in current weather and climate prediction systems are limited (Vitart et al., 2017). This limitation primarily stems from the quality of land surface reanalysis/assimilation data sets used to provide the land initial conditions for most dynamical models (Xue et al., 2021), which are still at a low level compared with the atmosphere and ocean surface reanalysis data sets (Li et al., 2024). What's more, due to the fast damping and chaotic nature of atmospheric dynamics in climate dynamical models (Du et al., 2023), it is still unclear how long the initial land conditions can influence the subseasonal prediction.

In particular, the land surface condition on the TP, which is one of the regions with the most active landatmosphere interaction, can strongly influence the TP local and global weather/climate across different timescales (Qiu, 2008; Wu et al., 2015; Xue et al., 2022). To examine the influence of land thermal condition over TP on the subseasonal prediction during boreal summer, several numerical studies have been taken in previous studies, which can be generally classified into two categories. One type of studies concentrates on how the TP land thermal condition, as lower boundary conditions, affect local and downstream extreme meteorological events at subseasonal timescale. These experiments are conducted by imposing land surface and subsurface variable perturbation/anomaly (e.g., anomalies of soil temperature from Qi et al., 2022; perturbation of key parameters that influence surface water and energy from Zhang, Sun, et al., 2024) over TP throughout the entire period of numerical simulation, which emphasized the effect of land surface condition as a lower boundary layer rather than the initial condition. The other type focuses on reporting the influence of land thermal initial condition over TP on subseasonal timescale. These studies demonstrated the role of TP initial land surface condition on regulating the downstream subseasonal prediction by carrying out numerical experiments/predictions by imposing  $\Delta T$  (land surface and subsurface temperature perturbation) at the first-time step of the model integration, based on the following three kinds of models. The first is regional modeling which are driven by reanalysis data as lateral boundary conditions rather than real-time predictions (e.g., Xu et al., 2022; Xue et al., 2018). The second is AMIP-type (Atmospheric Model Intercomparison Project) global atmospheric modeling, which utilized observed daily sea surface temperature (SST) and sea ice data as lower boundary condition throughout the model integration (e.g., Diallo et al., 2022; Oin et al., 2023), so that cannot represent the actual influence of land initial condition in real-time operational prediction owing to the chaotic influence of lower boundary condition. The third use fully coupled land-atmosphere-ocean models to make real-time operational prediction experiments under a recent research project named Impact of Initialized land surface temperature (LST) and Snowpack on Subseasonal to Seasonal Prediction (LS4P) (e.g., Ardilouze & Boone, 2023; Xue et al., 2023; Zhang, Pan, et al., 2024), but merely analyzed the case of June 2003 and reported the effect of TP land condition in late spring-early summer (pre-Mei-yu season). To this end, it has not been answered yet that whether and how long the TP initial land surface condition can influence the subseasonal rainfall prediction in peak summer (Mei-yu season), during which the extreme precipitation events frequently occur and cause severe disasters. Meanwhile, these previous studies have not concentrated on how the TP land initial thermal condition influence the evolution process of extreme rainfall.

In June–July 2020, the Yangtze River basin, Huaihe River basin, and parts of the Yellow River basin experienced a record-breaking Mei-yu rainfall (Liu & Ding, 2020). The accumulated precipitation amounts in 2020 Mei-yu season broke the historical record since 1961, causing numerous flood victims and huge economic losses (Gan, 2020). Previous studies have found that the record-breaking Mei-yu is primarily associated with the strong and westward extending Western Pacific Subtropical High (WPSH) (Ding et al., 2021), which is mainly aroused by the abnormal Indian Ocean warming (Tang et al., 2021) and the SST anomaly in the central and eastern Pacific (Pan et al., 2021). In addition, TP has also been found to play an important role in the development of the 2020 record-breaking Mei-yu rainfall. Zha and Wu (2022) found that a positive anomaly of snow cover over TP, associated with TP thermal forcing, persisted from winter to early summer in 2020. This positive anomaly can influence the Mei-yu rainfall in 2020 by intensifying the cold vortex over Northeast China as well as promoting the westward development of the WPSH. The activity of high potential vorticity system during the Mei-yu season in 2020, triggered by the abundant water vapor supply from the abnormal anticyclone over the northern Bay of Bengal, also played an important role in the extreme precipitation in that year (Ma et al., 2022).

Thus, aiming at the 2020 record-breaking Mei-yu rainfall, this study will investigate the effect of initial TP land thermal condition on the downstream subseasonal prediction, primarily based on the sensitive experiments of global climate ensemble prediction system FGOALS-f2. The remainder of this paper is organized as follows. Section 2 describes data sets, method and the prediction designs. An overview of extreme rainfall in July 2020 and associated TP thermal condition from observation are given in Section 3. Section 4 introduces the performance of 1-month lead prediction for 2020 Mei-yu in the operational prediction system. Section 5 proposes that how the initial TP thermal conditions influence the 2020 Mei-yu rainfall and associated mechanism based on prediction experiments. Finally, the conclusion and discussion will be given in Section 6.

### 2. Model Description, Data Sets and Methods

### 2.1. Observational Data and Methods

The observational 2479 in situ daily precipitation and surface temperature data, covering the period 1961–2020 in the mainland of China, were derived from the National Meteorological Information Center of the China Meteorological Administration. The daily atmospheric circulation fields in 1991-2020 were retrieved from the ERA5 data set provided by the European Center for Medium Range Weather Forecasts (ECMWF), with a 0.25° horizontal resolution and 32 pressure levels. In addition, the daily-mean land thermal fields over the TP region for the period of 1991-2020, including LST, subsurface temperature (SUBT), surface sensible heat flux (SHF) and surface latent heat flux, were also extracted from the ERA5 data set with a 0.25° horizontal resolution. The SUBT, generally corresponds to about 1–2 m soil thickness (Sellers et al., 1996), is represented by the soil temperature in ERA5 in this study that has four layers in the vertical direction with a top-down thickness of 0.07, 0.21, 0.72, and 1.89 m, respectively. The LST we used to choose the LST perturbation amount in Section 2.2 were extracted from 4 commonly used land assimilation/reanalysis data sets, including China Meteorological Administration Land Data Assimilation System products (CLDAS) (Shi et al., 2011), Global Land Data Assimilation System products (GLDAS) (Rodell et al., 2004), China Meteorological Administration (CRA40) (Liang et al., 2020), and ERA5. The potential vorticity (PV) budget is diagnosed in the isobaric coordinate system as follows in this study (Ertel, 1942; Hoskins et al., 1985):

$$PV = -g(\zeta + f)\frac{\partial \theta}{\partial p} \tag{1}$$

where  $(\zeta + f)$  represents the absolute vorticity  $\zeta$  and f are the relative vorticity and geostrophic vorticity respectively),  $\theta$  is potential temperature. The climatology of the observation and model data are calculated from 1991 to 2020 based on the 2479 in-situ daily precipitation data sets, ERA5 data set, and FGOALS-f2 prediction data, respectively.

### 2.2. Model Configurations and Experimental Design

The global climate ensemble prediction system used in this study is CAS-FGOALS-f2-V1.3. It was developed by the State Key Laboratory of Numerical Modeling for Atmospheric Sciences and Geophysical Fluid Dynamics (LASG) at the Institute of Atmospheric Physics (IAP), a part of the Chinese Academy of Sciences (CAS) (Bao et al., 2019; Fan et al., 2023; Li et al., 2021; Liu et al., 2023), and has been participated in the S2S Prediction Project Phase II. The horizontal resolution of FGOALS-f2 is about 100 km. FGOALS-f2 consists of four components: atmosphere, ocean, land surface, and sea ice. The atmospheric component is FAMIL2, which uses a finite-volume method (Lin, 2004) that discretized on a cube-sphere grid system (Putman & Lin, 2007). The key parameterization in FAMIL2 is a Convection Resolving Precipitation scheme (RCP), which is used to calculate the microphysics processes in the cumulus processes for both deep and shallow convection (Bao & Li, 2020). The oceanic and land surface component used in FGOALS-f2 are the Parallel Ocean Program, version 2 (POP2) (Kerbyson & Jones, 2005) and the Community Land Model, version 4 (CLM4.0) (Oleson et al., 2010), respectively. The sea ice component is the Los Alamos Sea Ice Model, version 4.0 (CICE4.0) (Hunke & Lipscomb, 2010). These four components are coupled by the coupler version 7 in the Community Earth System Model (Craig et al., 2012).

To test the contribution of initial land warming over TP to the downstream heavy rainfall in July 2020 in subseasonal timescale, we conducted one group of free run prediction experiment and two groups of sensitive prediction experiments with initial perturbation of LST and SUBT over TP. Each of these three prediction experiments comprises 16 ensemble members, which were generated for the hindcast based on a time-lag perturbation method. To generate the initial condition (27 June 2020) for numerical real-time prediction in this study, we use Newtonian nudging technique (Jeuken et al., 1996) to take reanalysis nudging from 1 January 1976 to the prediction start time (27 June 2020) with a 6-hr frequency, based on the CRA40 and Optimal Interpolation SST (OISST). After the initial field generation, we stopped the reanalysis nudging and initiate the free run of the model for the next 36 days, ending at 31 July 2020, to obtain a real prediction of July 2020. The only difference between the three experiments is the LST and SUBT over TP at the initial time of prediction. To emphasize the TP surface warming, we impose a negative LST and SUBT perturbation  $(-2^{\circ}C)$  in one sensible prediction experiment (hereafter the "TP\_C" run) and a positive one (+2°C) in the other (the "TP\_W" run) at the start time (00h 27th June 2020) (Figure S1 in Supporting Information S1). The perturbation amount (±2°C) in the sensitive experiments are chosen due to the following two aspects. The first is the amplitude for the year-to-year variation of TP LST, which is nearly 2°C measured by the standard deviation of LST over TP region during the past 20 years (2001–2020) (Figure S2 in Supporting Information S1). The second is the departure among different land assimilation/reanalysis data sets of TP LST, which are usually used to provide the land initial condition for most prediction systems (Xue et al., 2021). As shown in Figure S3 in Supporting Information S1, the deviation among four commonly used land assimilation/reanalysis data sets can reach up to 4°C during the initial dates of this prediction, which could represent the possible biases of initial surface temperature condition. The model climatology is computed from running the prediction system with the same starting day (27th June) following the setup described above during the 1991-2020 period.

## 3. Overview of Record-Breaking Mei-Yu in July 2020 and Associated TP Thermal Condition

The 2020 Mei-yu season with long duration (62 days) has a heavy accumulated precipitation (759.2 mm) over Yangtze-Huaihe River valley, which broke the historical record since 1961 (Ding et al., 2021). This record-breaking Mei-yu was comprised of multiple heavy precipitation processes which primarily occurred in July over the Middle and Lower Yangtze River Region (MLYR) (Chen et al., 2020). Based on observational precipitation data, the total rainfall over MLYR in July 2020 ranks the first since 1961 with 396.55 mm domain average accumulated precipitation (Figure 1a). Moreover, the domain averaged percentage of precipitation anomaly against the 1991–2020 climatology reached 100.6% in MLYR (Figure 1b).

Simultaneously, an evident land surface warming appeared over TP before the 2020 Mei-yu. It is found that The TP regional mean anomaly of sensible heat flux changes from -4.23 (W m<sup>-2</sup>) in March to +1.93 (W m<sup>-2</sup>) in June in 2020, denoting an increase of upward surface sensible heat flux in early summer (Figure 1c). Correspondingly, the surface temperature over TP evidently increased in early summer of 2020. As shown in Figure 1d,

21698996, 2024, 20, Downloaded from https://agupubs.onlinelibrary.wiley.com/doi/10.1029/2024JD041723 by Readcube-Labtiva, Wiley Online Library on [23/10/2024]. See the Terms and Conditions (https://onlinelibrary.

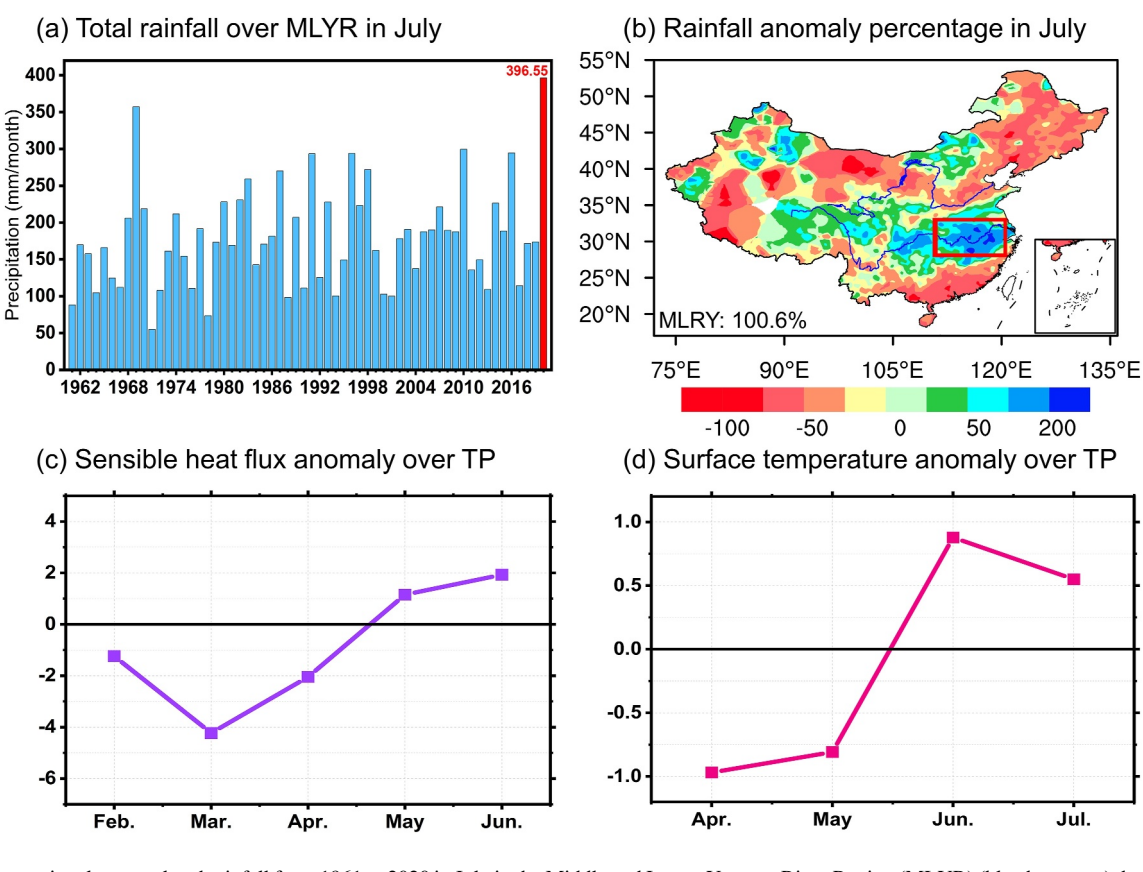


**Figure 1.** (a) Observational accumulated rainfall from 1961 to 2020 in July in the Middle and Lower Yangtze River Region (MLYR) (blue bars, mm) derived from CMA in-situ daily precipitation data. (b) Observational rainfall anomaly percentage in July 2020 (shading, %) derived from CMA in-situ daily data. (c) The temporal evolution of domain monthly mean sensible heat flux anomaly over TP from February to July in 2020 (line, W m<sup>-2</sup>, the positive value means the upward direction) derived from ERA5. (d) The temporal evolution of surface temperature anomaly over TP from April to July in 2020 (line, °C) derived from CMA in situ daily surface temperature data. The red bar and number in panel (a) denote the observational accumulated rainfall in 2020. The red rectangle in panel (b) represents the MLYR (111°–122°E, 28°–33°N). The numbers at the bottom left in panel (b) denote the MLYR domain-averaged percentage of precipitation anomaly.

the regional mean surface temperature anomaly over TP remained below  $0^{\circ}$ C in late spring and early summer, but shifted to a warm phase in June-July ( $-0.97^{\circ}$ C in April vs.  $+0.55^{\circ}$ C in July).

Considering the precursory anomalous land surface thermal condition over TP as described above, we subsequently conducted numerical experiments by modifying the surface temperature over TP in an operational prediction system depicted in the following sections.

# 4. One-Month Lead Prediction for 2020 Mei-Yu Rainfall in FGOALS-f2 Operational Prediction System

In order to examine the effect of initial surface thermal condition over TP on the prediction of Mei-yu rainfall in the following month (July 2020), three groups of prediction experiments with different initial thermal conditions over TP were employed. We first examine the performance of the 1-month lead prediction in the prediction experiment without initial LST and SUBT perturbation (called CTRL hereafter). Figures 2a and 2b have shown the percentage anomalies of precipitation in July 2020 derived from observation and CTRL, respectively. Compared with observation, the CTRL can roughly capture the location of main rain belt over MLYR in July 2020. However, the area-averaged percentage anomaly of rainfall is underestimated (100.6% in observation vs. 65.2% in prediction), and the maximum centers are mainly located over the north of Yangtze River in the CTRL rather than the south of Yangtze River in the observation. Consistent with the rainfall anomalies, the WPSH is enhanced and extended westward, and the associated low-level southwesterly anomaly can increase the conveying of water vapor into the MLYR region (Figures 2c and 2e). Meanwhile, the northeasterly anomalies, embedded in an anomalous cyclone over Northeast of China, increases the convergence over MLYR and

21698996, 2024, 20, Downloaded from https://agupubs.onlinelibrary.wiley.com/doi/10.1029/2024JD041723 by Readcube-Labtiva, Wiley Online Library on [23/10/2024]. See the Terms and Conditi

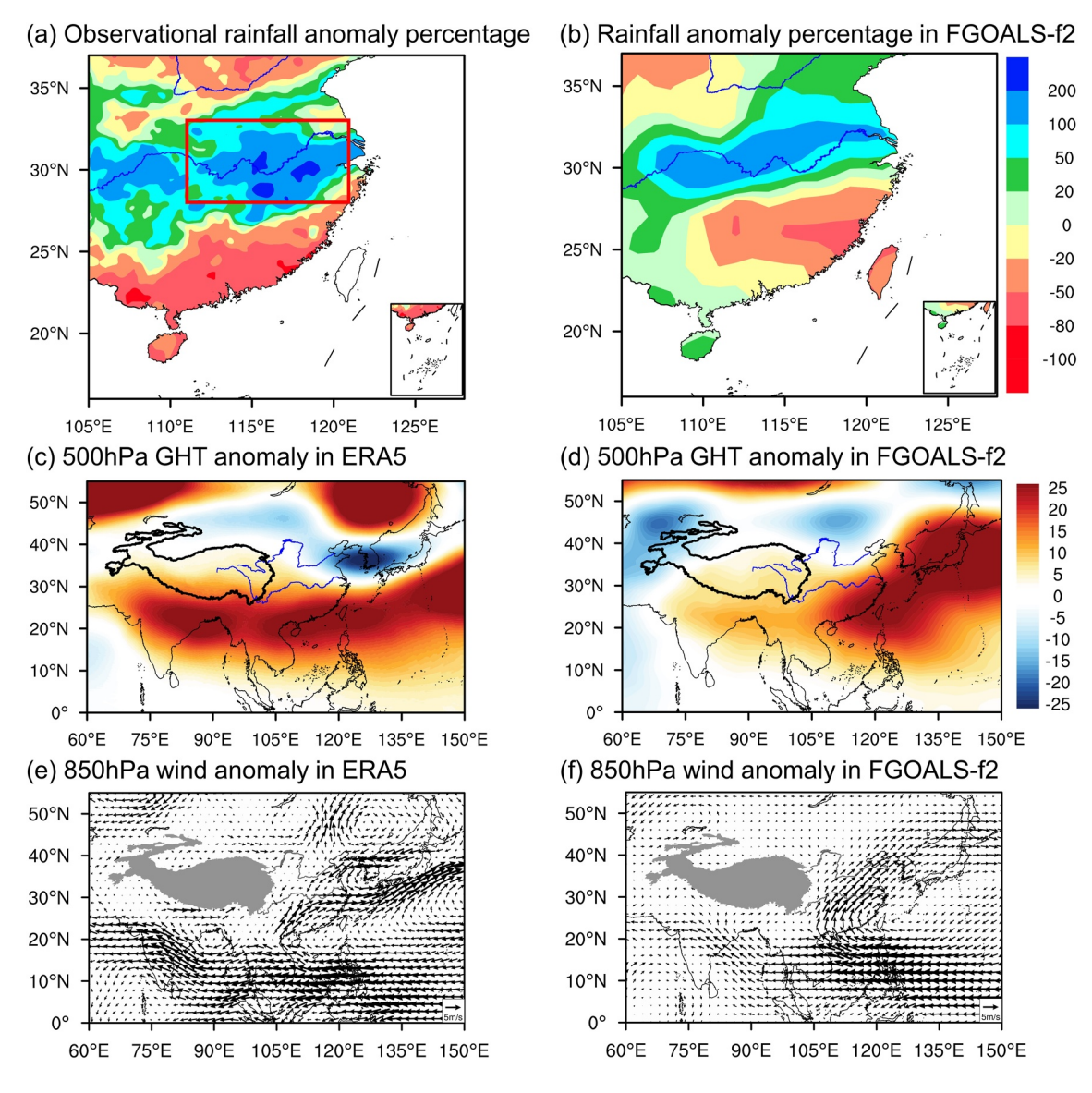


**Figure 2.** Rainfall anomaly percentage (shading, %) in July 2020 derived from panel (a) observation and (b) FGOALS-f2. Anomaly of 500 hPa geopotential height (shading, gpm) in July 2020 derived from panel (c) ERA5 and (d) FGOALS-f2. Anomaly of 850 hPa winds (vectors, m s<sup>-1</sup>) in July 2020 derived from panel (e) ERA5 and (f) FGOALS-f2. The red rectangle in panel (a) represents the MLYR.

enhances the upward motion through the invasion of cold air (Figures 2c and 2e). In comparison, the enhanced WPSH appears in CTRL but extends further northward. Accordingly, the anomalous cyclone does not occur over Northeast of China in CTRL (Figures 2d and 2f).

### 5. Initial Warming Over TP Increases the MLYR Rainfall in July 2020

According to the observational analysis in Section 3, a significant land surface warming appeared over TP in June prior to the occurring of extreme precipitation in MLYR during the 2020 Mei-yu season. To what extent and how the initial positive TP surface temperature anomaly influences the 2020 Mei-yu rainfall prediction in subseasonal prediction is worthwhile to be investigated. Hence, we conducted two groups of sensitive prediction experiments by imposing positive (+2°C) and negative (-2°C) initial LST and SUBT perturbations over TP (the "TP\_W" and "TP\_C"), respectively. The detailed prediction experiment designs are introduced in Section 2.2. In this section, we focus the differences between TP\_W and TP\_C from perspective of monthly mean, weekly mean, and day-by-day within the first week, aiming to emphasize the effect of TP thermal initial condition on monthly mean state, to identify how long the TP initial warming can impact the rainfall prediction, and to recognize the starting physical

21698996, 2024, 20, Downloaded from https://agupubs.onlinelibrary.wiley.com/doi/10.1029/2024JD041723 by Readcube-Labtiva, Wiley Online Library on [23/10/2024]. See the Terms and Conditional Conditio

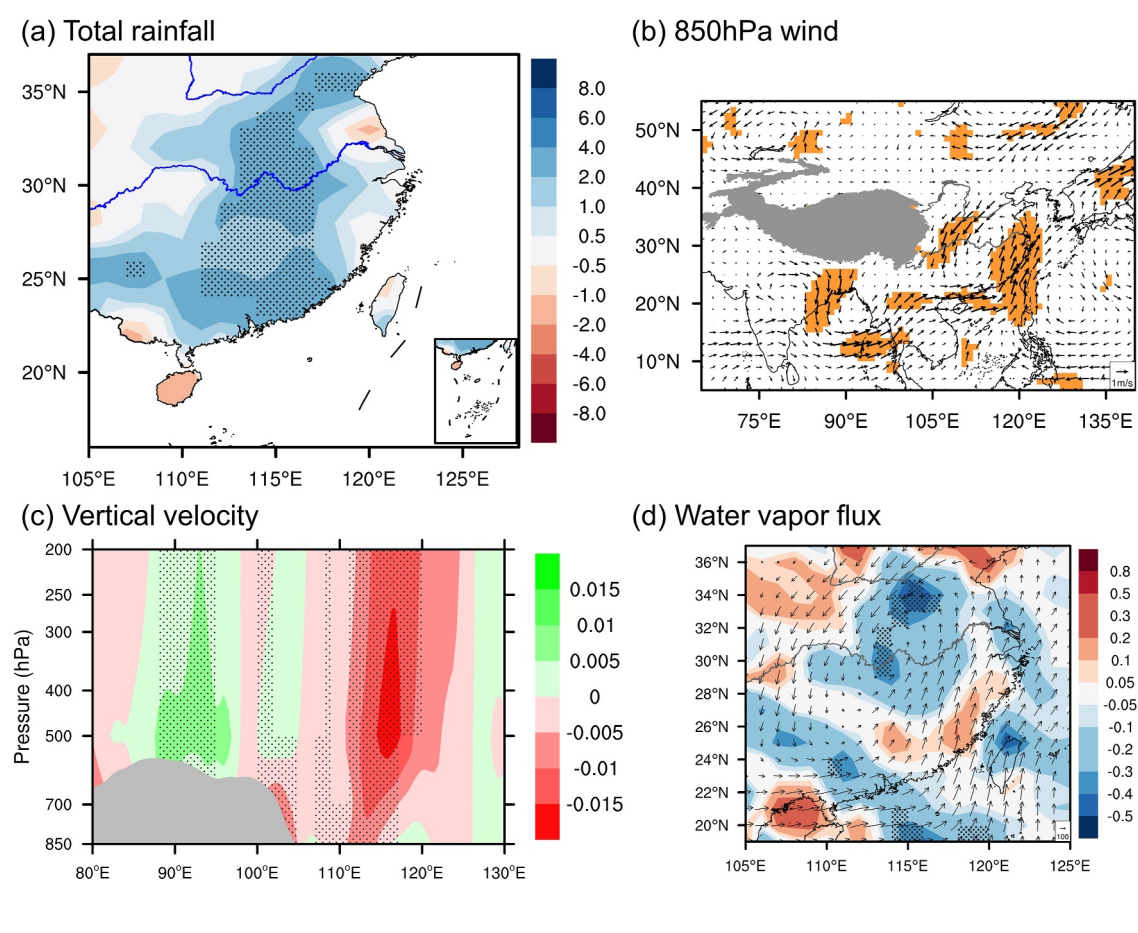


**Figure 3.** Monthly mean difference between TP\_C and TP\_W experiments in July 2020: (a) accumulated precipitation (shading, mm day $^{-1}$ ), (b) 850 hPa winds (vectors, m s $^{-1}$ ), (c) longitudinal–pressure cross section of vertical velocity between 25° and 38°N (Pa s $^{-1}$ , the negative value means ascending motion) and (d) 850 hPa vapor flux (vectors,  $10^{-5}$  kg m $^{-2}$  s $^{-1}$  hPa $^{-1}$ ) and its convergence/divergence (shading,  $10^{-7}$  kg m $^{-2}$  s $^{-1}$  hPa $^{-1}$ ). The black dots in panels (a, c, d) and the shading in panel (b) denote statistically significant at the 90% confidence level based on Student's *t*-test.

process that influence the downstream region, respectively. The statistical significance of the difference between two prediction experiments is assessed by *student's-t* test for paired samples. Here, the samples correspond to the 16 ensemble members of the prediction experiments. The null hypothesis is rejected for *p*-values exceeding 0.1, indicating that the differences between the two experiments are statistically significant at the 90% confidence level. And the results passing the *student's-t* test are considered as the statistically significant system that induced by the TP initial warming at the 90% confidence level, which influence the one-month-lead prediction.

Firstly, we analyzed the difference in monthly mean predictions between TP\_W and TP\_C (TP\_W monthly mean minus TP\_C monthly mean). As shown in Figure 3a, when the anomalous surface temperature over TP rises from -2°C to +2°C at the initial time of prediction (27th June), the predicted rainfall in July will significantly increase over MLYR (up to 3.2 mm day<sup>-1</sup>) and the south of China (up to 2.4 mm day<sup>-1</sup>). Correspondingly, with warmer initial condition over surface TP, a significant anomalous low-level cyclone emerges over eastern China in the prediction for July monthly mean (Figure 3b), accompanied by southwesterlies which facilities the transportation of warm water vapor from the Western Pacific and northern Indian Ocean into MLYR. Accordingly, significant low-level water vapor convergence and ascending motion can be seen over MLYR in 1-month lead prediction of TP\_W compared with TP\_C (Figures 3c and 3d), which are conducive to intensifying the downstream precipitation amplitude in July.

To further identify how long the TP initial warming impact the MLYR rainfall prediction, we make a comparison between the predictions in TP\_W and TP\_C week by week (TP\_W weekly mean minus TP\_C weekly mean). The results show that the low-tropospheric cyclone over eastern China, which is the most remarkable difference between two experiments in their 1-month lead predictions, has been already formed within the first week,

21698996, 2024, 20, Downloaded from https://agupubs.onlinelibrary.wiley.com/doi/10.1029/2024JD041723 by Readcube-Labtiva, Wiley Online Library on [23/10/2024]. See the Terms and Conditions (https://onlinelibrary.wiley

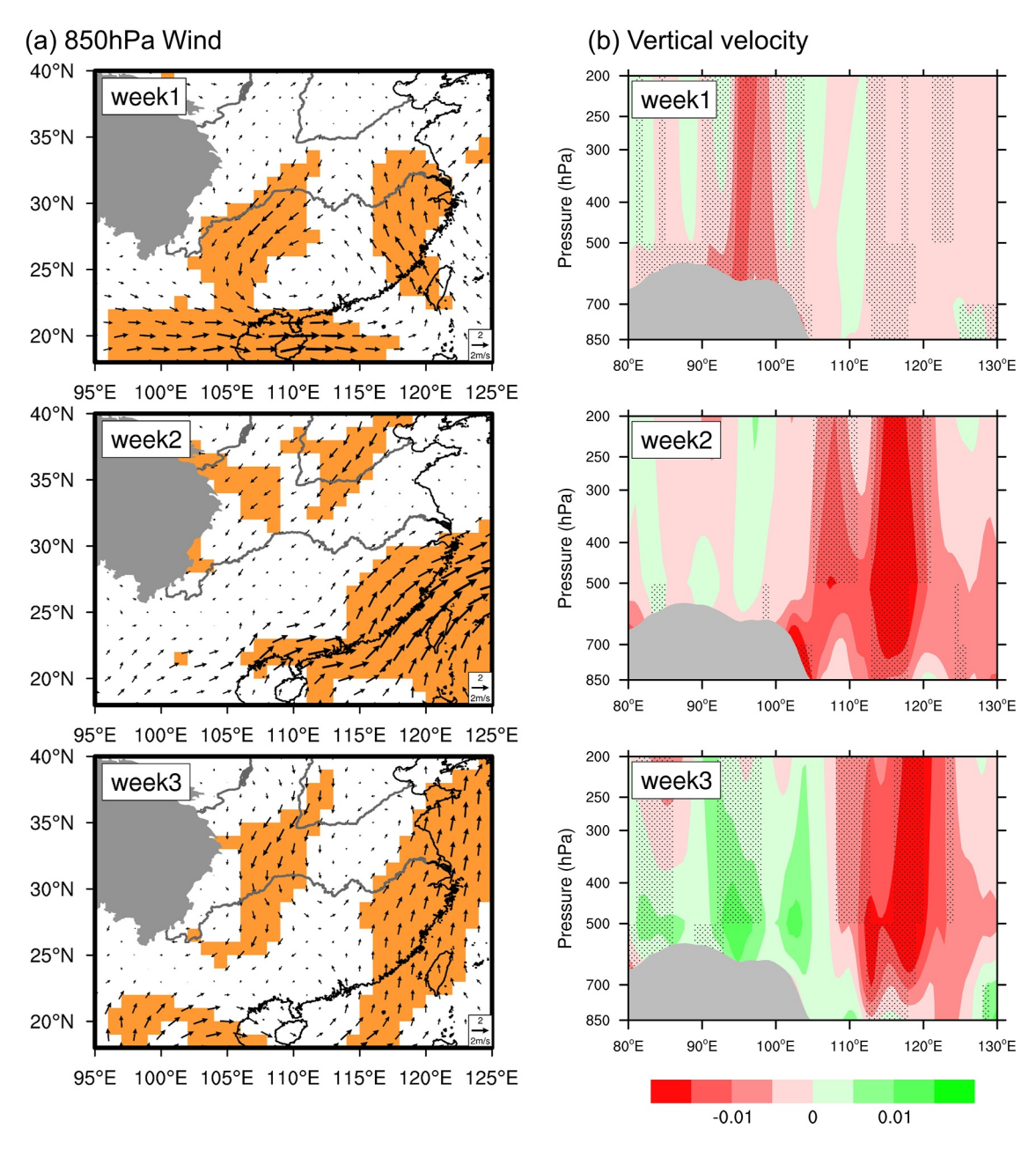


**Figure 4.** Weekly mean difference between TP-C and TP-W experiments with FGOALS-f2 for weeks 1–3 in July 2020: (a) 850 hPa winds (vectors, m s<sup>-1</sup>) and (b) the Longitudinal–pressure cross section of vertical velocity between 25° and 38°N (Pa s<sup>-1</sup>, the negative value means ascending motion). The shading in panel (a) and the black dots in panel (b) denote statistically significant at the 90% confidence level based on Student's *t*-test.

accompanied with the southerlies that are responsible for conveying warm water vapor to MLYR (Figure 4a). Consistently, a notable surge in upward motion can be seen over downstream in the 1-week prediction after the initial warming (Figure 4b), with the increase of rainfall in MLYR accordingly (Figure 5). The condensation latent heating released during the formation of precipitation can cause the positive feedback to support the ascending motion and enhance low-level convergence over MLYR (Sampe & Xie, 2010; Shen et al., 1986; Wang, 1987; Wu et al., 2020). Influenced by this positive feedback mechanism, the downstream cyclonic system along with ascending motion is strengthened in the second week of prediction and maintained till the third week of prediction (Figure 4a), indicating that the initial land warming over TP can impact the downstream rainfall prediction for 3 weeks in this prediction experiments.



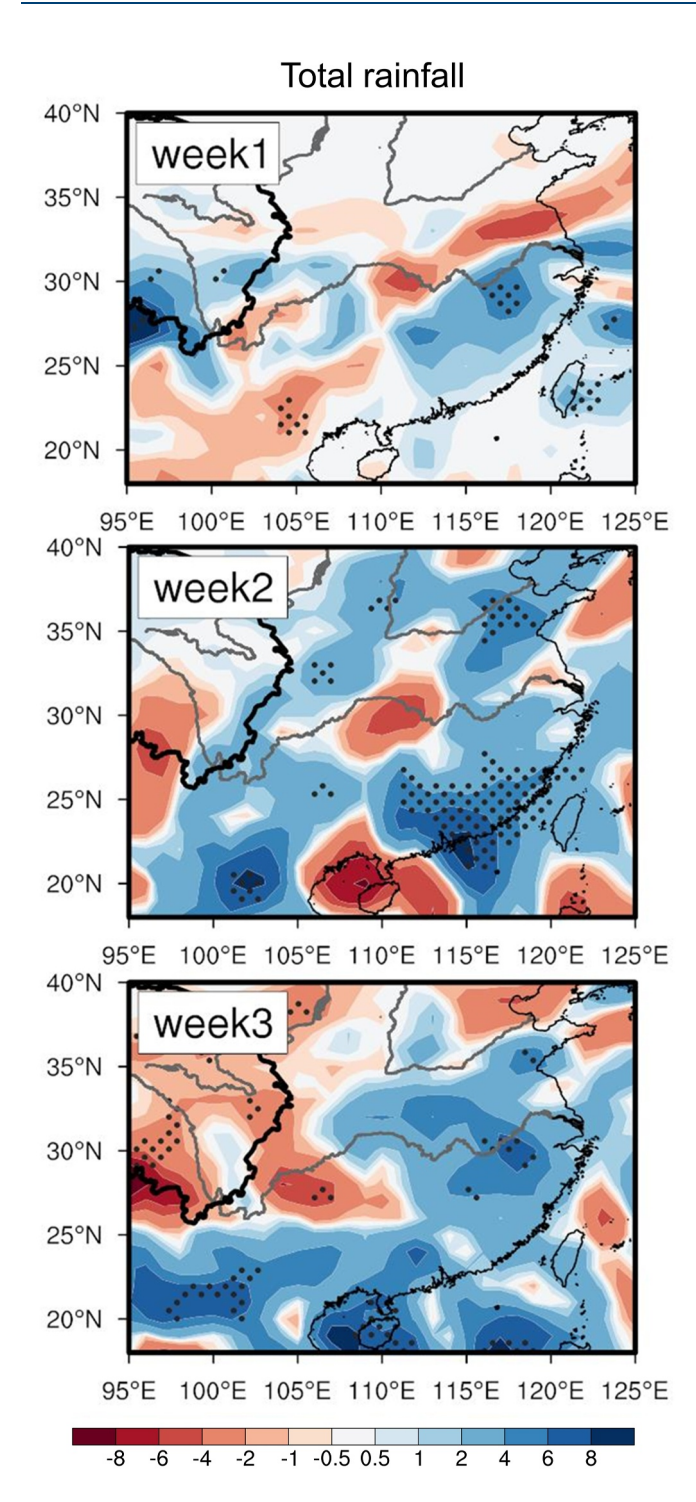


**Figure 5.** Weekly mean difference of accumulated precipitation (shading, mm) between TP\_C and TP\_W experiments with FGOALS-f2 for weeks 1–3 in July 2020. The black dots denote statistically significant at the 90% confidence level based on Student's *t*-test.

To further investigate how the downstream cyclone is generated within the first week of prediction, we made a day-by-day analysis for the 1-week prediction purposely borrowing potential vorticity (PV). PV is a synthetic meteorological quantity that can better represent both dynamical and thermodynamical properties of the atmosphere (Hoskins et al., 1985), which has been used widely in dynamic analysis of weather-climate systems (Hoskins, 1991). In particular, as the world's largest highland, TP is an evident PV source during summer and many previous studies use the PV theory to understand the variation of circulation systems over both the local and downstream of TP (He et al., 2022; Wu et al., 2020).

Figure 6 presents the evolution for PV and zonal-vertical winds  $(u, -\omega)$  during the period from the third day to sixth day (30th June to 3rd July) of prediction, averaged between 29° and 38°N of the latitudes. As a result, after imposing the positive LST and SUBT perturbations over TP at the initial time, a positive PV center associated with ascending motion is encountered over TP on the third day of prediction (30th June), owing to the increase of potential temperature vertical gradient between the land surface and the near-surface troposphere  $(\frac{\partial \theta}{\partial x})$ . Under the westerly flow in middle troposphere (Figure 7), this positive PV anomaly over TP gradually strengthening and eastward expanding on the 1st to 3rd July (Figures 6b-6d). Correspondingly, the noticeable positive PV along with the strong ascending motion significantly appeared in the middle-lower troposphere over downstream on the fourth day to sixth day of prediction (Figures 6b-6d), which indicates an increase in downstream low-level cyclonic vorticity and facilitates the development of low-level convergence. Consistent with above-mentioned PV evolution, the downstream low-level cyclone gradually develops in the first week of prediction (Figure 4a), which subsequently intensifies the rainfall amplitude over MLYR.

### 6. Summary and Discussion

Using two contrasting prediction experiments of a global climate model (FGOALS-f2), this work has demonstrated that changing the initial LST and SUBT over TP surface can significantly influence the 1-month lead prediction of rainfall over downstream Mei-yu rainfall in July 2020. As summarized in Figure 8, the initial land surface warming on TP firstly generates a near surface positive PV center over TP on the third day of prediction, which will gradually expand and propagate eastward along the background westerly flow in middle troposphere and amplified the low-level cyclonic vorticity over MLYR on the fourth to sixth day of prediction. Consequently, a low-level cyclone forms in the first week of prediction, with significant increase of rainfall over MLYR. Meanwhile, the positive feedback between the low-level cyclonic anomaly and the rainfall condensation latent heating facilitates the maintenance of the low-level cyclone and rainfall over MLYR for next 3 weeks in the prediction. The findings have confirmed the significant effect of TP initial thermal condition on downstream prediction ahead of 3 weeks during the peak summer (Mei-yu season), which is distinguishable from the previous studies that focus on the late spring-early summer (pre-Mei-yu season) (e.g., Diallo et al., 2022; Xue et al., 2023).

It should be noted that some previous works have shown that changing TP land initial thermal condition do not have a significant impact on MLYR in Mei-yu

season, which is different with our findings. For example, by imposing TP land surface and subsurface temperature perturbations around the initial time of simulation (22nd April–1st May, 2003), Xu et al. (2022) conducted four groups of sensitive numerical experiments based on a regional climate model, and reported that the changes of

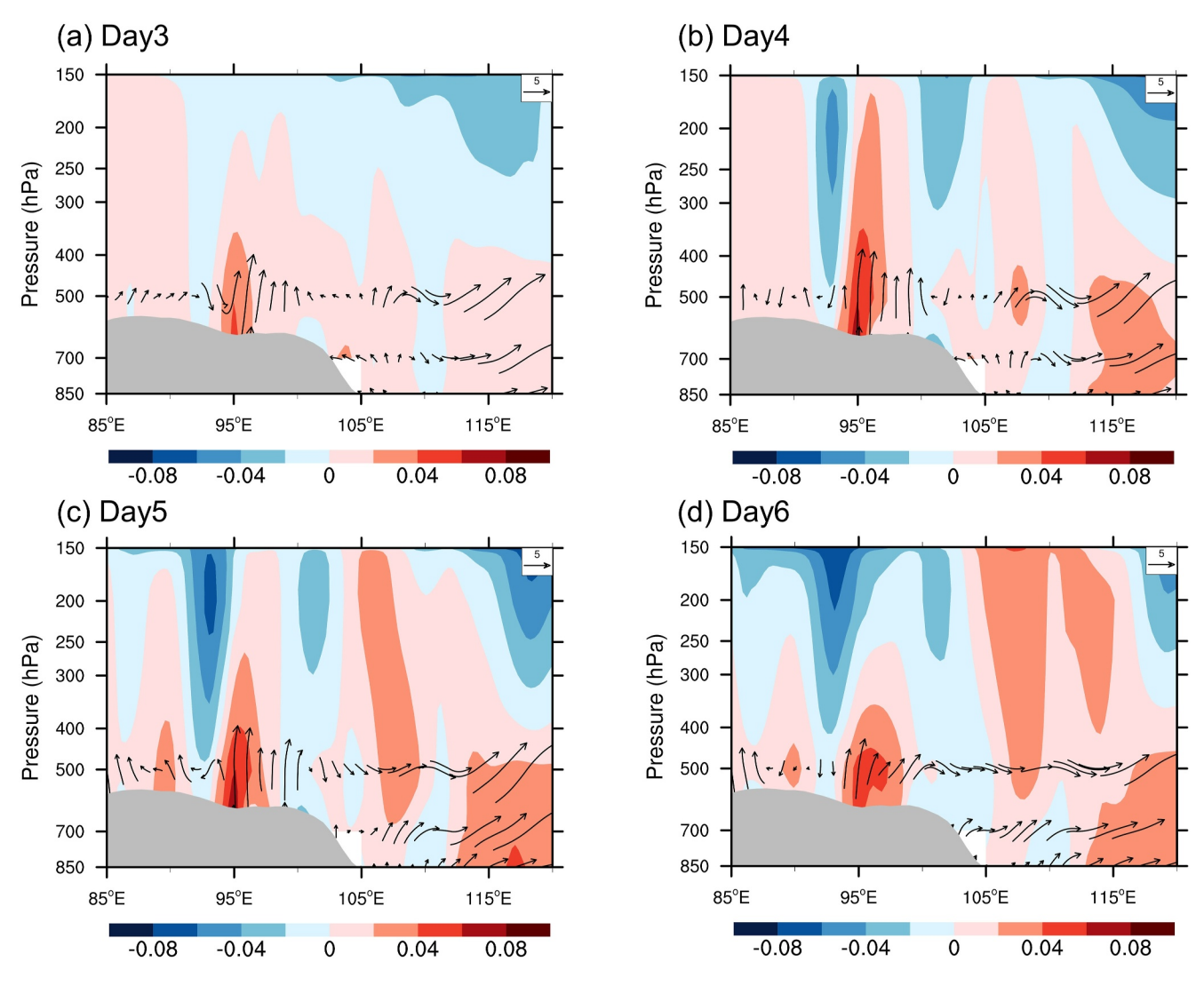


**Figure 6.** The longitudinal–pressure cross section (between 25° and 33°N) from 30th June to 3rd July (day 3–6) in 2020. Shadings are the daily mean difference of PV (PVU;  $1 \text{ PVU} = 10^{-6} \text{ K m}^2 \text{ s}^{-1} \text{ kg}^{-1}$ ) between TP-C and TP-W experiments with FGOALS-f2. Vectors are zonal–vertical circulations (zonal wind in m s<sup>-1</sup> and vertical motion multiplied by -100 in Pa s<sup>-1</sup>) in TP-W experiment.

rainfall, temperature, sensible and latent heat fluxes over MLYR are weak in July compared with in May, June and August by comparing the simulation results month-by-month from May to August. This may partly because that there exists a significant barrier in subseasonal forecast skill during the peak summer (Mei-yu season) for most dynamical models, since the abrupt transitional position of the western North Pacific subtropical and the rainy belt during this period (Yang et al., 2018). Intentionally, we investigated the differences of both the TP thermal surface condition and land-atmospheric coupling between pre-Mei-yu season (late spring-early summer) and Mei-yu season (peak summer). As shown Figure S4a in Supporting Information S1, the surface sensible heating over TP in Mei-yu season (90.7 W m<sup>-2</sup>) is stronger than that in pre-Mei-yu season (82.4 W m<sup>-2</sup>). Meanwhile, the strength of the land-atmosphere coupling over TP, measured by the land-air coupling intensity index (Dirmeyer, 2011), is increased by 50% from 2.2 in pre-Mei-yu season to 3.3 in Mei-yu season (Figure S4b in Supporting Information S1). The results have demonstrated that the land surface heating and the land-atmosphere coupling are much stronger in Mei-yu season than in pre-Mei-yu season. Moreover, it has been reported that the TP thermal conditions play an important role in modulating the atmospheric circulation and rainfall over East Asian region during the Mei-yu season, such as affecting the East Asia rainfall by arousing downstream low-level cyclonic anomaly (Fujinami & Yasunari, 2009). Therefore, the role of TP surface thermal initial condition is worthwhile to be concerned on the subseasonal prediction of East Asian climate during Mei-yu season.

21698996, 2024. 20, Downloaded from https://agupubs.onlinelibrary.wiley.com/doi/10.1029/2024JD041723 by Readeube-Labtiva, Wiley Online Library on [23/10/2024]. See the Terms

**Figure 7.** The 500 hPa PV and wind from 30th June to 3rd July (day 3–6) in 2020. The shadings are the daily mean difference of PV (PVU; 1 PVU =  $10^{-6}$  K m<sup>2</sup> s<sup>-1</sup> kg<sup>-1</sup>) between TP-C and TP-W experiments with FGOALS-f2. Vectors are 500 hPa zonal wind circulations (m s<sup>-1</sup>) in TP-W experiment. The black dots denote statistically significant at the 90% confidence level based on Student's *t*-test.

More studies need to be further investigated. First, the specific effect of land thermal condition would be verified using more summers. Second, the influence from other surface initial conditions is necessary to be investigated and compared among one another, including soil moisture (Wan et al., 2017) and snow cover (Li et al., 2018). Third, it is necessary to examine whether and how improving the land thermal condition using real observation combined with some specific assimilation method (e.g., nudging, Four-Dimensional Variation, Ensemble Kalman Filter) are conductive to the regional subseasonal prediction.

elibrary.wiley.com/terms-and-conditions) on Wiley Online Library for rules of use; OA articles are governed by the applicable Creati

21698996, 2024, 20, Downloaded from https://agupubs.onlinelibrary.wiley.com/doi/10.1029/2024JD041723 by Readcube-Labtiva, Wiley Online Library on [23/10/2024]. See the Terms and Conditions (https://onlinelibrary.wiley.com/term

and-conditions) on Wiley Online Library for rules of use; OA articles

**Figure 8.** Schematic diagram for demonstrating how the surface initial warming over TP impact the rainfall prediction over MLYR in July 2020 in subseasonal timescale. (a) Stage 1: The TP surface warming at the initial time of prediction (27th June) generates a positive PV center over the TP surface atmosphere during the third day of prediction. (b) Stage 2: In the first week of prediction, eastward moving positive vorticity amplifies the low-level cyclonic vorticity over downstream. Consequently, a low-level cyclone forms over MLYR, with significant increase of rainfall. (c) Stage 3: Positive feedback between the low-level cyclone and middle-tropospheric latent heating helps to maintain the low-level cyclone and rainfall over MLYR for 3 weeks in the prediction.

### **Conflict of Interest**

The authors declare no conflicts of interest relevant to this study.

### **Data Availability Statement**

The ERA5 data can be accessed on https://cds.climate.copernicus.eu/cdsapp#!/dataset/reanalysis-era5-pressure-levels-monthly-means?tab=form. The observational station daily precipitation and surface temperature data derived from CMA can be accessed on https://www.researchgate.net/publication/383529117\_CMA\_in-situ. The CLDAS data derived from CMA can be accessed on https://www.researchgate.net/publication/383529509\_CLDAS\_LST. The GLDAS data can be accessed on https://disc.gsfc.nasa.gov/datasets/GLDAS\_NOAH025\_

3H\_2.1/summary?keywords=GLDAS. The CRA40 data derived from CMA can be accessed on https://www.researchgate.net/publication/383530963\_CRA40\_LST.

### Acknowledgments

This study was supported by funding from the National Natural Science Foundation of China (Grants 42475022, 42261144671, 91737306). This research would like to thank the support from Anling Liu and Yuxian Pan.

### References

- Amenu, G. G., Kumar, P., & Liang, X. (2005). Interannual variability of deep-layer hydrologic memory and mechanisms of its influence on surface energy fluxes. *Journal of Climate*, 18(23), 5024–5045. https://doi.org/10.1175/JCL13590.1
- Ardilouze, C., & Boone, A. A. (2023). Impact of initializing the soil with a thermally and hydrologically balanced state on subseasonal predictability. Climate Dynamics, 62(4), 2629–2644. https://doi.org/10.1007/s00382-023-07024
- Bao, Q., & Li, J. (2020). Progress in climate modeling of precipitation over the Tibetan plateau. *National Science Review*, 7(3), 486–487. https://doi.org/10.1093/nsr/nwaa006
- Bao, Q., Wu, X. F., Li, J. X., Wang, L., He, B., Wang, X. C., et al. (2019). Outlook for El Niño and the Indian Ocean dipole in autumn-winter 2018–2019. Chinese Science Bulletin, 64(1), 73–78. (in Chinese). https://doi.org/10.1360/N972018-00913
- Chen, T., Zhang, F. H., Yu, C., Ma, J., Zhang, X. D., Shen, X. L., et al. (2020). Synoptic analysis of extreme Mei-yu precipitation over Yangtze River basin during JuneJuly 2020. *Meteorological Monthly*, 46(11), 1415–1426. (in Chinese with English abstract). https://doi.org/10.7519/j.issn.1000-0526.2020.11.003
- Craig, A. P., Vertenstein, M., & Jacob, R. (2012). A new flexible coupler for earth system modeling developed for CCSM4 and CESM1. *The International Journal of High Performance Computing Applications*, 26(1), 31–42. https://doi.org/10.1177/1094342011428141
- Diallo, I., Xue, Y., Chen, Q., Ren, Q., & Guo, W. (2022). Effects of spring Tibetan Plateau land temperature anomalies on early summer floods/droughts over the monsoon regions of South East Asia. Climate Dynamics, 62(4), 1–23. https://doi.org/10.1007/s00382-021-06053-8
- Ding, Y., Liu, Y., & Hu, Z. Z. (2021). The record-breaking Mei-yu in 2020 and associated atmospheric circulation and tropical SST anomalies. Advances in Atmospheric Sciences, 38(12), 1980–1993. https://doi.org/10.1007/s00376-021-0361-2
- Dirmeyer, P. A. (2011). The terrestrial segment of soil moisture–climate coupling. Geophysical Research Letters, 38(16), L16702. https://doi.org/10.1029/2011GL048268
- Dirmeyer, P. A., Gentine, P., Ek, M. B., & Balsamo, G. (2019). Land surface processes relevant to sub-seasonal to seasonal (S2S) prediction. In A. W. Robertson & F. Vitart (Eds.), Sub-seasonal to seasonal prediction—The gap between weather and climate forecasting (pp. 165–181). https://doi.org/10.1016/B978-0-12-811714-9.00008-5
- Du, D., Subramanian, A. C., Han, W., Wei, H.-H., Sarojini, B. B., Balmaseda, M., & Vitart, F. (2023). Assessing the impact of ocean in situ observations on MJO propagation across the maritime continent in ECMWF subseasonal forecasts. *Journal of Advances in Modeling Earth Systems*, 15(2), e2022MS003044. https://doi.org/10.1029/2022MS003044
- Ertel, H. (1942). Ein neuer hydrodynamischer wirbelsatz. Meteorologische Zeitschrift, 59, 277–281.
- Fan, Y., Yang, J., Li, J., Qi, X., & Bao, Q. (2023). Gain of one-month lead predicting spring rainfall over China: A comparison between FGOALS-f2 ensemble prediction system and its driving stretched-grid downscaling prediction system. Atmospheric Research, 283, 106570. https://doi.org/10.1016/j.atmosres.2022.106570
- Fu, S.-M., Zhang, Y.-C., Wang, H.-J., Tang, H., Li, W.-L., & Sun, J.-H. (2022). On the evolution of a long-lived mesoscale convective vortex that acted as a crucial condition for the extremely strong hourly precipitation in Zhengzhou. *Journal of Geophysical Research: Atmospheres*, 127(11), e2021JD036233, https://doi.org/10.1029/2021JD036233
- Fujinami, H., & Yasunari, T. (2009). The effects of midlatitude waves over and around the Tibetan plateau on submonthly variability of the East Asian summer monsoon. *Monthly Weather Review*, 137(7), 2286–2304. https://doi.org/10.1175/2009MWR2826.1
- Gan, N. (2020). China has just contained the coronavirus. Now it's battling some of the worst floods in decades. CNN. Retrieved from https://edition.cnn.com/2020/07/14/asia/china-flood-coronavirus-intl-hnk/index.html
- He, B., Sheng, C., Wu, G., Liu, Y., & Tang, Y. (2022). Quantification of seasonal and interannual variations of the Tibetan Plateau surface thermodynamic forcing based on the potential vorticity. *Geophysical Research Letters*, 49(5), e2021GL097222. https://doi.org/10.1029/ 2021GL097222
- He, S., Knudsen, E. M., Thompson, D. W. J., & Furevik, T. (2018). Evidence for predictive skill of high-latitude climate due to midsummer sea ice extent anomalies. *Geophysical Research Letters*, 45(17), 9114–9122. https://doi.org/10.1029/2018GL078281
- Hoskins, B. J. (1991). Towards a PV-θ view of the general circulation. *Tellus*, 43AB(4), 27–35. https://doi.org/10.1034/j.1600-0870.1991.t01-3-00005.x
- Hoskins, B. J., Mcintyre, M. E., & Robertson, A. W. (1985). On the use and significance of isentropic potential vorticity maps. *Quarterly Journal of the Royal Meteorological Society*, 111(470), 877–946. https://doi.org/10.1256/smsqj.47001
- Hunke, E. C., & Lipscomb, W. H. (2010). CICE: The Los Alamos Sea ice model documentation and software user's manual version 4.1. Tech. Rep. LA-CC-06-012 (p. 675).
- IPCC. (2021). Climate change 2021: The physical science basis. Contribution of Group I to the sixth assessment report of the intergovernmental panel on climate change. Retrieved from https://www.ipcc.ch/report/ar6/wgl/downloads/report/IPCC\_AR6\_WGI\_Full\_Report.pdf
- Jeuken, A. B. M., Siegmund, P. C., Heijboer, L. C., Feichter, J., & Bengtsson, L. (1996). On the potential of assimilating meteorological analyses in a global climate model for the purpose of model validation. *Journal of Geophysical Research*, 101(D12), 16939–16950. https://doi.org/10. 1029/96jd01218
- Kerbyson, D. J., & Jones, P. W. (2005). A performance model of the Parallel Ocean Program. IJHPCA, 19(3), 261–276. https://doi.org/10.1177/1094342005056114
- Koster, R. D., Mahanama, S. P. P., Yamada, T. J., Balsamo, G., Berg, A. A., Boisserie, M., et al. (2010). Contribution of land surface initialization to subseasonal forecast skill: First results from a multi-model experiment. Geophysical Research Letters, 37(2), L02402. https://doi.org/10.1029/2009GL041677
- Koster, R. D., Suarez, M. J., Liu, P., Jambor, U., Berg, A., Kistler, M., et al. (2004). Realistic initialization of land surface states: Impacts on subseasonal forecast skill. *Journal of Hydrometeorology*, 5(6), 1049–1063. https://doi.org/10.1175/JHM-387.1
- Lesk, C., Rowhani, P., & Ramankutty, N. (2016). Influence of extreme weather disasters on global crop production. *Nature*, 529(7584), 84–87. https://doi.org/10.1038/nature16467
- Li, J., Bao, Q., Liu, Y., Wu, G., Wang, L., He, B., et al. (2021). Dynamical seasonal prediction of tropical cyclone activity using the FGOALS-f2 ensemble prediction system. Weather and Forecasting, 36(5), 1759–1778. https://doi.org/10.1175/WAF-D-20-0189.1
- Li, W., Guo, W., Qiu, B., Xue, Y., Hsu, P.-C., & Wei, J. (2018). Influence of Tibetan Plateau snow cover on East Asian atmospheric circulation at medium-range time scales. *Nature Communications*, 9(1), 4243. https://doi.org/10.1038/s41467-018-06762-5





### Journal of Geophysical Research: Atmospheres

- 10.1029/2024JD041723
- Li, X., Liu, F., Ma, C., Hou, J., Zheng, D., Ma, H., et al. (2024). Land data assimilation: Harmonizing theory and data in land surface process studies. *Reviews of Geophysics*, 62(1), e2022RG000801. https://doi.org/10.1029/2022RG000801
- Liang, P., & Lin, H. (2018). Sub-seasonal prediction over East Asia during boreal summer using the ECCC monthly forecasting system. *Climate Dynamics*, 50(3–4), 1007–1022. https://doi.org/10.1007/s00382-017-3658-1
- Liang, X., Jiang, L. P., Pan, Y., Shi, C., Liu, Z., & Zhou, Z. (2020). A 10-yr global land surface reanalysis interim dataset (CRA-Interim/Land): Implementation and preliminary evaluation. *Journal of Meteorological Research*, 34(1), 101–116. https://doi.org/10.1007/s13351-020-9083-0 Lin, S. (2004). A "Vertically Lagrangian" finite-volume dynamical core for global models. *Monthly Weather Review*, 132(10), 2293–2307. https://doi.org/10.1175/1520-0493(2004)132<2293:AVLFDC>2.0.CO;2
- Liu, A., Yang, J., Bao, Q., He, B., Wu, X., Liu, J., et al. (2023). Subseasonal-to-seasonal prediction of arctic sea ice using a fully coupled dynamical ensemble forecast system. *Atmospheric Research*, 295, 107014. https://doi.org/10.1016/j.atmosres.2023.107014
- dynamical ensemble forecast system. *Atmospheric Research*, 293, 10/014. https://doi.org/10.1016/j.atmosres.2023.10/014

  Liu, Y., Xue, Y., Li, Q., Lettenmaier, D., & Zhao, P. (2020). Investigation of the variability of near-surface temperature anomaly and its causes over the Tibetan plateau. *Journal of Geophysical Research: Atmospheres*, 125(19), e2020JD032800. https://doi.org/10.1029/2020JD032800
- Liu, Y. Y., & Ding, Y. H. (2020). Characteristics and possible causes for the extreme Mei-yu in 2020. Meteorological Monthly, 46(11), 1393–1404. (in Chinese with English abstract). https://doi.org/10.7519/j.issn.1000-0526.2020.11.001
- Ma, T., Wu, G., Liu, Y., & Mao, J. (2022). Abnormal warm sea-surface temperature in the Indian Ocean, active potential vorticity over the Tibetan Plateau, and severe flooding along the Yangtze River in summer 2020. Quarterly Journal of the Royal Meteorological Society, 148(743), 1001– 1019. https://doi.org/10.1002/qj.4243
- Mariotti, A., Ruti, P. M., & Rixen, M. (2018). Progress in subseasonal to seasonal prediction through a joint weather and climate community effort. Npj Climate and Atmospheric Science, 1, 4. https://doi.org/10.1038/s41612-018-0014-z
- O'Gorman, P. A. (2015). Precipitation extremes under climate change. Current Climate Change Reports, 1, 49–59. https://doi.org/10.1007/s40641-015-0009-3
- Oleson, W. B., Lawrence, M., Bonan, B., Flanner, G., Kluzek, E., Lawrence, J., et al. (2010). Technical description of version 4.0 of the community land model (CLM). NCAR/TN-478+STR, 173pp. https://doi.org/10.5065/D6FB50WZ
- Pan, X., Li, T., Sun, Y., & Zhu, Z. W. (2021). Cause of extreme heavy and persistent rainfall over Yangtze River in summer 2020. Advances in Atmospheric Sciences, 38(12), 1994–2009. https://doi.org/10.1007/s00376-021-0433-3
- Putman, W. M., & Lin, S.-J. (2007). Finite-volume transport on various cubed-sphere grids. *Journal of Computational Physics*, 227(1), 55–78. https://doi.org/10.1016/j.jcp.2007.07.022
- Qi, X., & Yang, J. (2019). Extended-range prediction of a heat wave event over the Yangtze River valley: Role of intraseasonal signals. Atmospheric and Oceanic Science Letters, 12(6), 451–457. https://doi.org/10.1080/16742834.2019.1669408
- Qi, X., Yang, J., Xue, Y., Bao, Q., Wu, G., & Ji, D. (2022). Subseasonal warming of surface soil enhances precipitation over the eastern Tibetan Plateau in early summer. *Journal of Geophysical Research: Atmospheres*, 127(23), e2022JD037250. https://doi.org/10.1029/2022JD037250
- Qin, Y., Tang, Q., Xue, Y., Liu, Y., & Lin, Y. (2023). Improved subseasonal–to– seasonal precipitation prediction of climate models with nudging approach for better initialization of Tibetan Plateau–Rocky Mountain Circumglobal wave train and land surface conditions. *Climate Dynamics*, 62(4), 2645–2657. https://doi.org/10.1007/s00382-023-07082-1
- Qiu, J. (2008). The third pole. *Nature*, 454(7203), 393–396. https://doi.org/10.1038/454393a
- Robertson, A. W., Kumar, A., Peña, M., & Vitart, F. (2015). Improving and promoting subseasonal to seasonal prediction. Bulletin of the American Meteorological Society, 96(3), ES49–ES53. https://doi.org/10.1175/BAMS-D-14-00139.1
- Rodell, M., Houser, P., Jambor, U., Gottschalck, J., Mitchell, K., Meng, C. J., et al. (2004). The global land data assimilation system. *Bulletin of the American Meteorological Society*, 85(3), 381–394. https://doi.org/10.1175/bams-85-3-381
- Sampe, T., & Xie, S. P. (2010). Large-scale dynamics of the Meiyu-Baiu rainband: Environmental forcing by the westerly jet. *Journal of Climate*, 23(1), 113–134. https://doi.org/10.1175/2009JCLI3128.1
- Sellers, P. J., Randall, D. A., Collatz, G. J., Berry, J. A., Field, C. B., Dazlich, D. A., et al. (1996). A revised land surface parametrization (SiB2) for atmospheric GCMs. Part I: Model formulation. *Journal of Climate*, 9(4), 676–705. https://doi.org/10.1175/1520-0442(1996)009<0676: arlspf>2.0.co;2
- Seneviratne, S. I., Corti, T., Davin, E. L., Hirschi, M., Jaeger, E. B., Lehner, I., et al. (2010). Investigating soil moisture–climate interactions in a changing climate: A review. *Earth-Science Reviews*, 99(3–4), 125–161. https://doi.org/10.1016/j.earscirev.2010.02.004
- Shen, R., Reiter, E. R., & Bresch, J. F. (1986). Numerical simulation of the development of vortices over the Qinghai-Xizang (Tibet) plateau.

  Meteorology and Atmospheric Physics, 35(1–2), 70–95. https://doi.org/10.1007/BF01029526
- Shi, C., Xie, Z., Qian, H., Liang, M., & Yang, X. (2011). China land soil moisture EnKF data assimilation based on satellite remote sensing data. Science China Earth Sciences, 54(9), 1430–1440. https://doi.org/10.1007/s11430-010-4160-3
- Sobolowski, S., Gong, G., & Ting, M. (2010). Modeled climate state and dynamic responses to anomalous North American snow cover. *Journal of Climate*, 23(3), 785–799. https://doi.org/10.1175/2009JCLI3219.1
- Tang, S. L., Luo, J.-J., He, J. Y., Wu, J. Y., Zhou, Y., & Ying, W. S. (2021). Toward understanding the extreme floods over Yangtze River valley in June–July 2020: Role of tropical oceans. Advances in Atmospheric Sciences, 38(12), 2023–2039. https://doi.org/10.1007/s00376-021-1036-8
- Vitart, F., Ardilouze, C., Bonet, A., Brookshaw, A., Chen, M., Codorean, C., et al. (2017). The subseasonal to seasonal (S2S) prediction project database. *Bulletin of the American Meteorological Society*, 98(1), 163–173. https://doi.org/10.1175/BAMS-D-16-0017.1
- Wan, B., Gao, Z., Chen, F., & Lu, C. (2017). Impact of Tibetan plateau surface heating on persistent extreme precipitation events in southeastern China. *Monthly Weather Review*, 145(9), 3485–3505. https://doi.org/10.1175/mwr-d-17-0061.1
- Wang, B. (1987). The development mechanism for Tibetan plateau warm vortices. *Journal of the Atmospheric Sciences*, 44(20), 2978–2994. https://doi.org/10.1175/1520-0469(1987)044<2978:TDMFTP>2.0.CO;2
- Wei, K., Ouyang, C. J., Duan, H. T., Li, Y. L., Chen, M. X., Ma, J., et al. (2020). Reflections on the catastrophic 2020 Yangtze River basin flooding in southern China. *Innovation*, 1(2), 100038. https://doi.org/10.1016/j.xinn.2020.100038
- White, C. J., Franks, S. W., & McEvoy, D. (2015). Using subseasonal-to-seasonal (S2S) extreme rainfall forecasts for extended-range flood prediction in Australia. Proceedings of the International Association of Hydrological Sciences, 370, 229–234. https://doi.org/10.5194/piahs-370-229-2015
- Wu, B., & Francis, J. A. (2019). Summer arctic cold anomaly dynamically linked to East Asian heat waves. *Journal of Climate*, 32(4), 1137–1150. https://doi.org/10.1175/JCLI-D-18-0370.1
- Wu, G., Ma, T., Liu, Y., & Jiang, Z. (2020). PV-Q perspective of cyclogenesis and vertical velocity development downstream of the Tibetan Plateau. *Journal of Geophysical Research: Atmospheres*, 125(16), e2019JD030912. https://doi.org/10.1029/2019JD030912
- Wu, G. X., Duan, A. M., Liu, Y. M., Mao, J. Y., Ren, R. C., Bao, Q., et al. (2015). Tibetan plateau climate dynamics: Recent progress and outlook. National Science Review, 2(2), 100–116. https://doi.org/10.1093/nsr/nwu045





## Journal of Geophysical Research: Atmospheres

- 10.1029/2024JD041723
- Xu, H., Liang, X.-Z., & Xue, Y. (2022). Regional climate modeling to understand Tibetan heating remote impacts on East China precipitation. Climate Dynamics, 62(4), 2683–2701. https://doi.org/10.1007/s00382-022-06266-5
- Xue, Y., Diallo, I., Boone, A. A., Yao, T., Zhang, Y., Zeng, X., et al. (2022). Spring land temperature in Tibetan plateau and global-scale summer precipitation: Initialization and improved prediction. Bulletin America Meteorology Social, 103(12), E2756–E2767. https://doi.org/10.1175/BAMS-D-21-0270.1
- Xue, Y., Diallo, I., Boone, A. A., Zhang, Y., Zeng, X., Lau, W. K., et al. (2023). Remote effects of Tibetan plateau spring land temperature on global subseasonal to seasonal precipitation prediction and comparison with effects of sea surface temperature: The GEWEX/LS4P phase I experiment. Climate Dynamics, 62(4), 1–26. https://doi.org/10.1007/s00382-023-06905-5
- Xue, Y., Diallo, I., Li, W., David Neelin, J., Chu, P. C., Vasic, R., et al. (2018). Spring land surface and subsurface temperature anomalies and subsequent downstream late spring-summer droughts/floods in North America and East Asia. *Journal of Geophysical Research: Atmospheres*, 123(10), 5001–5019. https://doi.org/10.1029/2017JD028246
- Xue, Y., Yao, T., Boone, A. A., Diallo, I., Liu, Y., Zeng, X., et al. (2021). Impact of initialized land surface temperature and snowpack on subseasonal to seasonal prediction project, phase I (LS4PI): Organization and experimental design. Geoscientific Model Development, 14(7), 4465–4494. https://doi.org/10.5194/gmd-14-4465-2021
- Yamada, T. J., & Pokhrel, Y. (2019). Effect of human-induced land disturbance on subseasonal predictability of near-surface variables using an atmospheric general circulation model. Atmosphere, 10(11), 725. https://doi.org/10.3390/atmos10110725
- Yang, J., Zhu, T., Gao, M., Lin, H., Wang, B., & Bao, Q. (2018). Late-July barrier for subseasonal forecast of summer daily maximum temperature over Yangtze River Basin. Geophysical Research Letters, 45(22), 12610–12615. https://doi.org/10.1029/2018GL080963
- Yeh, T.-C., Wetherald, R. T., & Manabe, S. (1984). The effect of soil moisture on the short-term climate and hydrology change–a numerical experiment. *Monthly Weather Review*, 112(3), 474–490. https://doi.org/10.1175/1520-0493(1984)112<0474:Teosmo>2.0.Co;2
- Zha, P., & Wu, Z. (2022). Contribution of the Tibetan plateau snow cover to the record-breaking rainfall over the Yangtze River valley in June 2020. Atmosphere-Ocean, 61(2), 122–134. https://doi.org/10.1080/07055900.2022.2151408
- Zhang, Q., Sun, G., Dai, G., & Mu, M. (2024). Impact of uncertainties in land surface processes on subseasonal predictability of heat waves onset over the Yangtze River Valley. *Journal of Geophysical Research: Atmospheres*, 129(1), e2023JD038674. https://doi.org/10.1029/2023JD038674
- Zhang, Y., Pan, Y., Xue, Y., Diallo, I., Zeng, X., Li, S., et al. (2024). Near-global summer circulation response to the spring surface temperature anomaly in Tibetan Plateau—The GEWEX/LS4P first phase experiment. Climate Dynamics, 62(4), 2907–2924. https://doi.org/10.1007/s00382-024-07210-5
- Zhou, B., & Qian, J. (2021). Changes of weather and climate extremes in the IPCC AR6. Climate Change Research, 17(6), 713e718. (Chinese). https://doi.org/10.12006/j.issn.1673-1719.2021.167